Original Article

The combination of ^{18}F-fluorodeoxyglucose and ^{18}F 9-fluoropropyl-(+)-dihydrotetrabenazine positron emission tomography for distinguishing between early-onset and late-onset idiopathic Parkinson disease and analyzing influencing factors

Shuang Li[1,2,3,4], Weizhao Lu[1,3,4], Shaozhen Yan[1,3,4], Tianbin Song[1,3,4], Chun Zhang[1,3,4], Chang Yang[1,3,4], Jie Lu[1,3,4]

[1]Department of Radiology and Nuclear Medicine, Xuanwu Hospital, Capital Medical University, Beijing, China; [2]Department of Nuclear Medicine, Xiangyang No. 1 People's Hospital, Hubei University of Medicine, Xiangyang, China; [3]Beijing Key Laboratory of Magnetic Resonance Imaging and Brain Informatics, Beijing, China; [4]Key Laboratory of Neurodegenerative Diseases, Ministry of Education, Beijing, China

Contributions: (I) Conception and design: S Li; (II) Administrative support: J Lu; (III) Provision of study materials or patients: T Song, C Zhang; (IV) Collection and assembly of data: S Li, C Yang; (V) Data analysis and interpretation: W Lu, S Yan; (VI) Manuscript writing: All authors; (VII) Final approval of manuscript: All authors.

Correspondence to: Jie Lu, MD, PhD. Department of Radiology and Nuclear Medicine, Xuanwu Hospital, Capital Medical University, No. 45 Chuangchun Road, Xicheng District, Beijing 100053, China; Beijing Key Laboratory of Magnetic Resonance Imaging and Brain Informatics, Beijing, China; Key Laboratory of Neurodegenerative Diseases, Ministry of Education, Beijing, China. Email: imaginglu@hotmail.com.

Background: The classification of Parkinson disease by age of onset has proven to be a valuable method for subtyping, given its practical application in clinical settings. However, the interactions between the metabolic brain changes, dopaminergic dysfunction, and clinical manifestations in patients with early-onset (early-iPD) and late-onset (late-iPD) idiopathic Parkinson disease have not been adequately evaluated. Therefore, this study aimed to investigate the difference in cerebral metabolism and presynaptic dopaminergic function between patients with early-iPD and those with late-onset disease using ^{18}F-fluorodeoxyglucose (^{18}F-FDG) and [^{18}F] 9-fluoropropyl-(+)-dihydrotetrabenazine (^{18}F-FP-DTBZ) positron emission tomography (PET). Furthermore, the goal was to further explore the correlation between imaging measurements and clinical manifestations in the early and late idiopathic patients with Parkinson disease.

Methods: This cross-sectional study included 80 patients with idiopathic Parkinson disease and 29 healthy control participants who underwent ^{18}F-FDG and^{18}F-FP-DTBZ PET imaging at Xuanwu Hospital, Capital Medical University from August 2022 to August 2023. The patients were categorized into early-iPD (n=27) and late-iPD (n=53) groups based on an age threshold of 50 years. The mean standardized uptake value of ^{18}F-FDG and the standardized uptake value ratio (SUVR) of ^{18}F-FP-DTBZ were compared between the early-iPD and late-iPD groups using unpaired Student *t*-tests. Furthermore, pairwise correlations among cerebral metabolism, dopaminergic function, and corresponding clinical ratings in all patients were conducted using Pearson correlation analysis.

Results: Patients with late-iPD exhibited a significant metabolic decrease in the frontal, parietal, and temporal cortex, along with the globus pallidus, putamen, thalamus, and cerebellum, compared to those with early-iPD in ^{18}F-FDG PET imaging (all P values <0.05). Furthermore, the ^{18}F-FP-DTBZ binding potential was significantly lower in the contralateral caudate and anterior putamen of patients with late-iPD compared to those with early-iPD (contralateral caudate: 3.16±1.2 *vs.* 2.63±0.7, P=0.020; contralateral anterior putamen: 2.49±1.2 *vs.* 2.05±0.7, P=0.040). Further analysis of the correlations between imaging clinical features revealed that glucose metabolism increases and dopaminergic function decreases with higher motor ratings.

© AME Publishing Company.

Conclusions: ^{18}F-FDG and ^{18}F-FP-DTBZ PET offer an objective molecular imaging basis for distinguishing between early-onset and late-onset idiopathic with Parkinson disease. Additionally, correlation analysis between imaging and clinical data represents a new approach for exploring the potential applications in future studies involving patients with early-iPD and late-iPD.

Keywords: ^{18}F-fluorodeoxyglucose positron emission tomography (^{18}F-FDG PET); [^{18}F] 9-fluoropropyl-(+)-dihydrotetrabenazine PET (^{18}F-FP-DTBZ PET); early-onset; late-onset; Parkinson disease

Submitted Apr 21, 2024. Accepted for publication Aug 29, 2024. Published online Sep 26, 2024.
doi: 10.21037/qims-24-804
View this article at: https://dx.doi.org/10.21037/qims-24-804

Introduction

Parkinson disease is a chronic age-related neurodegenerative disease which affects over 6 million individuals globally. There has been a 2.5-fold increase in its prevalence over the past 30 years, positioning Parkinson disease as a prominent contributor to neurological disability (1,2). Nigrostriatal dopaminergic denervation and the presence of intraneuronal aggregates of α-synuclein (or *Lewy bodies*) is the neuropathological hallmark of Parkinson disease (3). Extensive loss of nigral neurons is characteristic of Parkinson disease and can lead to a significant reduction in the abundance of presynaptic dopamine transporter (4). Individuals with Parkinson disease have a combination of motor symptoms such as bradykinesia, rigidity, and tremor, and non-motor features such as constipation, hyposmia, depression, cognitive decline, and sleep disturbances, which adversely impacts their quality of life and increases the burden of caregivers (5).

The classification of Parkinson disease by age of onset has proven to be a valuable method for subtyping, given its practical application in clinical settings (6,7). Early-onset idiopathic Parkinson disease (early-iPD) refers to the clinical diagnosis of Parkinson disease occurring before the age of 50 years (8) and exhibits clinical characteristics that differ from those of late-onset idiopathic Parkinson disease (late-iPD) (9). Patients with early-iPD typically have a lower risk of experiencing cognitive deficits, a higher prevalence of levodopa-associated dyskinesia, and a slower rate of disease progression (10). Conversely, individuals with late-iPD demonstrate more significant dopaminergic dysfunction and more severe motor and non-motor symptoms, resulting in accelerated disease advancement (11). Consequently, understanding the relationship between age of onset, metabolism, and the clinical features of Parkinson disease could provide valuable insights into the disease and offer new perspectives in understanding the characteristic manifestations in early-iPD and late-iPD.

However, few studies have explored the correlations between cerebral metabolism, dopaminergic function, and the clinical manifestations in patients with early-iPD and late-iPD. Previous molecular imaging studies have examined the interactions among cerebral metabolism changes, dopaminergic dysfunction, and clinical manifestations using the ^{18}F-fluorodeoxyglucose (^{18}F-FDG) and [^{18}F] 9-fluoropropyl-(+)-dihydrotetrabenazine (^{18}F-FP-DTBZ) positron emission tomography (PET) imaging in patients with Parkinson disease (12). Additionally, a recent study suggested that reduced dopamine transporter binding in early-iPD anticipates the future emergence of motor complications. However, this phenomenon does not correlate with the severity of motor symptoms, highlighting the presence of age-related variations in the striatal compensatory mechanisms among individuals with Parkinson disease (13).

However, these abovementioned studies did not directly evaluate the interactions between the metabolic brain changes, dopaminergic dysfunction and clinical manifestations in patients with early-iPD and late-iPD. We therefore conducted a dual-tracer PET study using both ^{18}F-FDG and ^{18}F-FP-DTBZ PET imaging in a cohort of 27 patients with early-iPD and 53 with late-iPD. We aimed to characterize the cerebral metabolism, dopaminergic function, and the clinical manifestations of patients with early-iPD and late-iPD. We present this article in accordance with the STROBE reporting checklist (available at https://qims.amegroups.com/article/view/10.21037/qims-24-804/rc).

© AME Publishing Company.

Methods

Participants

Eighty patients diagnosed with idiopathic Parkinson disease by two senior specialists in movement disorders according to the Movement Disorder Society PD criteria (14,15) and scanned with both ^{18}F-FDG and ^{18}F-FP-DTBZ PET were consecutively enrolled in this study between August 2022 and August 2023. The patients were divided into the early-iPD group (n=27; age of onset between 21 and 50 years; 15 males and 12 females; 44.0±7.7 years) and late-iPD group (n=53; age of onset >50 years; 34 males and 19 females; 64.6±6.5 years). In addition, the study included 29 healthy controls (HCs) divided into two subgroups to match patients with Parkinson disease in demographic characteristics and age during ^{18}F-FDG and ^{18}F-FP-DTBZ PET scans. This retrospective study was conducted in accordance with the Declaration of Helsinki (as revised in 2013) and was approved by the Medical Research Ethics Committee of Xuanwu Hospital, Capital Medical University (No. [2023]044). The requirement for written informed consent was waived due to the retrospective nature of the analysis.

Study design

All participants fasted overnight and discontinued antiparkinsonian medications for a minimum of 12 hours before undergoing clinical evaluation and imaging under two distinct modalities. The assessment included the application of the Unified Parkinson Disease Rating Scale (UPDRS) (16,17) and determination of the Hoehn and Yahr (H&Y) stage (18). Subsequently, all ^{18}F-FDG PET imaging was applied in all participants, and ^{18}F-FP-DTBZ PET imaging was applied the following day.

Data acquisition

All participants were examined using a hybrid 3.T PET-magnetic resonance imaging (MRI) scanner (uPMR790, United Imaging Healthcare, Shanghai, China) equipped with a 24-channel head/neck coil. During ^{18}F-FDG PET imaging (150–200 MBq), scans were acquired over 45 to 55 minutes after injection. Additionally, ^{18}F-FP-DTBZ PET imaging involved acquiring scans about 90 minutes after an intravenous injection of ^{18}F-FP-DTBZ (222 MBq). The imaging acquisitions for each patient took place in a quiet, dimly lit room while the patient was in a resting state.

PET images were reconstructed using the ordered subset expectation maximization (OSEM) algorithm during a 24-minute scan (4 iterations and 20 subsets incorporating time of flight and point spread function) under the following parameters: matrix size =256×256, field of view (FOV) = 300×300 mm, and voxel size =2.4×2.4×2.8. Structural MRI images were obtained using a three-dimensional T1-weighted (3D T1WI) sequence under the following parameters: repetition time =7.86 ms, echo time =3.8 ms, number of slices =176 slices, voxel size =1.0×1.0×1.0 mm^3, and FOV =256×256 mm.

Image analysis

Quantitative analysis of cerebral metabolism

In the analysis of ^{18}F-FDG PET images, each participant's PET image was coregistered to their structural T1 images, and individual structural images were spatially normalized into template brain space with a default PET template in MM BrainAnalysis software (United Imaging Intelligence Co., Ltd., Shanghai, China) and then smoothed. Initial segmentation of the 3D T1 MRI sequence into gray matter, white matter, and cerebrospinal fluid was followed by further segmentation into 106 brain regions. The segmentation results of T1 were mapped onto the PET images, from which the mean standardized uptake value (SUV_{mean}) for each cerebral cortex was derived (19).

Quantitative analysis of dopaminergic function

Two physicians with over 5 years of experience in neural system PET diagnosis jointly conducted a semiquantitative analysis of the striatal ^{18}F-FP-DTBZ uptake index. They interpreted the images without knowledge of the patients' diagnoses. The region of interest (ROI) was delineated on the fusion image using the PET post-processing workstation. Initially, MR images at the striatal level were selected and displayed to trace the bilateral putamen and caudate nucleus on each image. These tracings were then transferred to the corresponding PET images to determine the average radioactivity of the putamen and caudate nucleus on each side (20). The occipital cortex served as the reference region for calculating the binding ratio for each ROI. The standardized uptake value ratio (SUVR) was determined by dividing the uptake in the target ROIs by that in the reference area (21,22). In the Parkinson disease group, the contralateral ROIs were delineated as those brain regions opposite to the predominantly affected limbs and were analyzed independently from the ipsilateral ROIs.

© AME Publishing Company.

Table 1 Demographic and clinical characteristics of all participants

Clinical feature	Young HCs (n=12)	Older HCs (n=17)	Early-iPD (n=27)	Late-iPD (n=53)	P_1	P_2	P_3
Sex (M/F)	7/5	9/8	15/12	34/19	>0.99	0.568	0.477
Age (years)	43.1±9.2	64.1±6.9	43.1±6.8	64.6±6.5	0.992	0.752	<0.001*
Age at onset (years)	–	–	40.7±9.7	61.8±6.7			<0.001*
Disease duration (years)	–	–	3.7±3.6	2.8±2.0			0.155
Education (years)	–	–	11.8±3.7	12.2±3.6			0.755
Total UPDRS score	–	–	33.5±7.9	51.7±18.4			0.037*
UPDRS III	–	–	26.2±11.7	26.7±14.5			0.917
H&Y stage	–	–	2.06±0.5	2.0±0.8			0.780
MMSE score	–	–	28.7±2.5	26.7±3.4			0.020*
MoCA score	–	–	25.4±3.5	22.6±5.0			0.032*

The data are presented as the mean ± standard deviation. P_1 indicates the P value for the comparison of the young HC and early-iPD groups. P_2 indicates the P value for the comparison of the older HC and late-iPD groups. P_3 indicates the P value for the comparison of the early-iPD and late-iPD groups. *, statistically significant differences (P<0.05). HC, healthy control; early-iPD, early-onset idiopathic Parkinson disease; late-iPD, late-onset idiopathic Parkinson disease; iPD, idiopathic Parkinson disease; M/F, male/female; UPDRS III, Unified Parkinson Disease Rating Scale Part III; H&Y stage, Hoehn-Yahr stage; MMSE, Mini-Mental State Examination; MoCA, Montreal Cognitive Assessment.

Meanwhile, in the HC group, the average values of regional SUVR from both sides were computed for comparison purposes.

Statistical analysis

Statistical analysis was performed using the Student *t*-test and Mann-Whitney test (two-tailed) to assess quantitative variables, which are expressed as the mean and standard deviation (SD). Meanwhile, qualitative variables are represented as frequency and proportion. We compared the demographics between the early-iPD and late-iPD groups. The SUV_{mean} of the ^{18}F-FDG in the whole brain and the SUVR of ^{18}F-FP-DTBZ in the striatum between the early-iPD and late-iPD groups were compared with unpaired Student *t*-tests. Furthermore, comparisons between the early-iPD and late-iPD groups in terms of cerebral metabolism, dopaminergic function, and UPDRS motor ratings across various H&Y stages were conducted using analysis of variance (ANOVA) with Bonferroni corrections for multiple comparisons. Correlations between cerebral metabolism, dopaminergic function, and related clinical motor ratings in all patients were evaluated through Pearson correlation coefficient analysis. Statistical analyses were carried out using SPSS 25 (IBM Corp., Armonk, NY, USA), with statistical significance set at a two-tailed P value of less than 0.05.

Results

Clinical and demographic characteristics

The clinical and demographic characteristics of 80 patients with idiopathic Parkinson disease (23 patients with early-iPD and 57 with late-iPD) and those of 29 HCs are presented in *Table 1* and *Figure 1*. No significant differences were observed in sex or age between the HC group and the idiopathic Parkinson disease group. Furthermore, no significant disparities in sex, education, UPDRS III, disease duration, or H&Y stage were found between the early-iPD and late-iPD groups. However, notable differences were evident in age at onset, age, total UPDRS score, Mini-Mental State Examination (MMSE) score, and Montreal Cognitive Assessment (MoCA) score. Post hoc analysis revealed that the late-iPD group exhibited a significantly worse total UPDRS, MMSE, and MoCA scores compared to the early-iPD group (all P values <0.05).

Cerebral metabolism characteristics of the early-iPD, late-iPD, and HC groups

Patients with early-iPD exhibited notable increased

© AME Publishing Company.

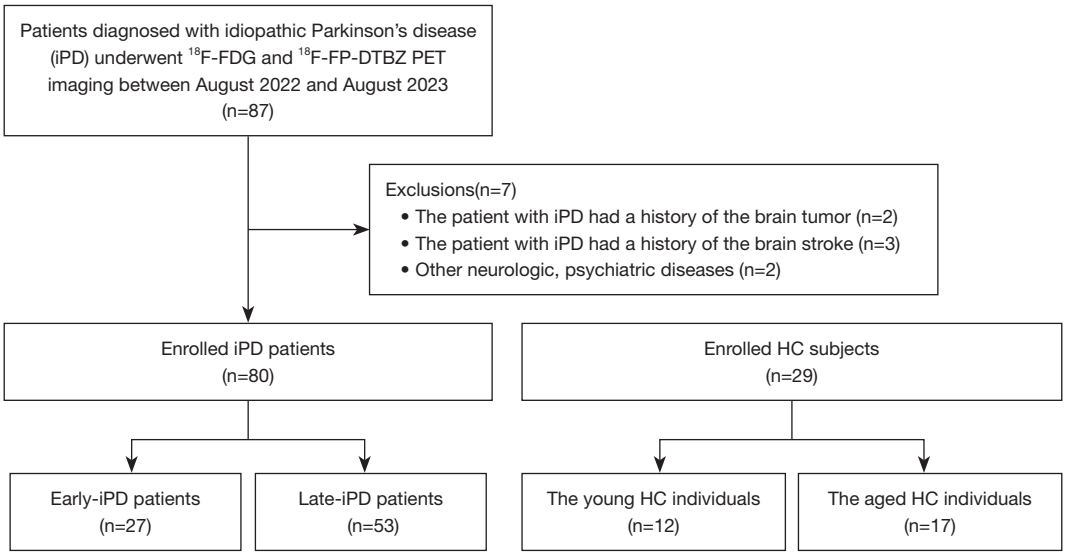

Figure 1 Patient selection flowchart. ^{18}F-FDG, ^{18}F-fluorodeoxyglucose; ^{18}F-FP-DTBZ, [^{18}F] 9-fluoropropyl-(+)-dihydrotetrabenazine; PET, positron emission tomography; early-iPD, early-onset idiopathic Parkinson disease; late-iPD, late-onset idiopathic Parkinson disease; HC, healthy control.

metabolism in the globus pallidus, putamen, thalamus, pons, and cerebellum as compared to the young HCs (all P values <0.05). Compared with the older HC individuals, patients with late-iPD exhibited significant metabolic reduction in the frontal, parietal, and temporal cortex, in addition to markedly increased metabolism in the globus pallidus and putamen (all P values <0.05). Additionally, as compared to patients with early-iPD, patients with late-iPD had significant metabolic reduction in the frontal, parietal, and temporal cortex and in the globus pallidus, putamen, thalamus, and cerebellum (all P values <0.05). The comparisons of cerebral metabolism on ^{18}F-FDG between patients the early-iPD, those late-iPD, and HC groups are presented in *Table 2* and *Figure 2*.

Presynaptic dopaminergic function characteristics in the early-iPD, late-iPD, and HC groups

In the comparison with the HC group, there was reduced ^{18}F-FP-DTBZ uptake in the bilateral caudate, anterior putamen, and posterior putamen in the early-iPD group (contralateral: 5.30±1.6 *vs.* 1.76±0.7, P<0.001; ipsilateral: 5.30±1.6 *vs.* 1.59±0.6, P<0.001) and late-iPD group (contralateral: 4.93±1.6 *vs.* 1.59±0.8, P<0.001; ipsilateral: 4.93±1.6 *vs*, 1.87±0.9, P<0.001), with a more pronounced reduction in the posterior putamen. Furthermore, the ^{18}F-FP-DTBZ binding potential was significantly lower in the contralateral caudate and anterior putamen of patients with late-iPD compared to those with early-iPD (contralateral caudate: 3.16±1.2 *vs.* 2.63±0.7, P=0.020; contralateral anterior putamen: 2.49±1.2 *vs.* 2.05±0.7, P=0.040). A significant decline in ^{18}F-FP-DTBZ uptake was also observed in the bilateral posterior putamen, with no significant differences between the early-iPD and late-iPD groups. The comparisons of presynaptic dopaminergic function between early-iPD, late-iPD, and HC groups are presented in *Table 3* and *Figures 2*,*3*.

Changes in PET imaging measurements and motor rating

In patients with early-iPD, there were significant increases in SUV_{mean} with higher H&Y stages in ^{18}F-FDG PET imaging according to ANOVA (putamen: F=5.146, P=0.007; globus pallidus: F=3.620, P=0.034). Additionally, the striatum regional ^{18}F-FP-DTBZ uptake decreased with higher H&Y stage according to ANOVA (caudate: F=9.228, P<0.001; anterior putamen: F=9.577, P<0.001; posterior putamen: F=4.916, P=0.012). Furthermore, there was a significant increase in UPDRS III scores with higher H&Y stage according to ANOVA (F=4.553; P=0.032) (*Table 4*).

In patients with late-iPD, ^{18}F-FDG PET imaging demonstrated a significant increase in cerebral glucose

© AME Publishing Company.

Table 2 The characteristics of ^{18}F-FDG PET imaging in the early-iPD, late-iPD, and HC groups

Region	SUV_{mean}				P_1	P_2	P_3
	Young HC	Older HC	Early-iPD	Late-iPD			
Frontal cortex	8.27±1.7	8.18±1.7	8.03±1.9	6.40±2.6	0.707	0.010※	0.005*$
Parietal cortex	7.89±2.7	8.05±1.8	7.51±1.6	6.42±2.5	0.561	0.015※	0.043*
Temporal cortex	6.38±1.0	6.78±1.5	7.20±1.60	5.73±2.09	0.115	0.028※	0.002*$
Globus pallidus	6.01±0.8	5.11±1.0	6.94±1.30	5.93±1.93	0.010※	0.017※	0.001*$
Putamen	7.61±0.9	6.55±0.7	9.79±1.93	8.09±3.43	0.001※	0.011※	0.001*$
Thalamus	6.40±0.8	6.11±0.8	7.82±1.57	6.55±2.34	0.005※	0.449	0.013*
Pons	4.43±0.5	4.51±0.7	5.16±1.00	4.60±1.45	0.019※	0.806	0.078
Cerebellum	5.38±0.7	5.36±0.9	6.77±1.51	5.88±1.91	0.004※	0.286	0.038*

The data are presented as the mean ± standard deviation. P_1 indicates the P value for the comparison of the young HC and early-iPD groups. P_2 indicates the P value for the comparison of the older HC and late-iPD groups. P_3 indicates the P value for the comparison of the early-iPD and late-iPD groups. ※, P<0.05 versus HC group; *, P<0.05 versus early-iPD group; $, P<0.01 versus early-iPD group (ANOVA: Bonferroni test). ^{18}F-FDG, ^{18}F-fluorodeoxyglucose; PET, positron emission tomography; early-iPD, early-onset idiopathic Parkinson disease; late-iPD, late-onset idiopathic Parkinson disease; SUVmean, the mean standardized uptake value; HC, healthy control.

metabolism with higher H&Y stage according to ANOVA (putamen: F=3.190, P=0.046; globus pallidus: F=3.807, P=0.026). Furthermore, there was a decrease in regional ^{18}F-FP-DTBZ uptake in caudate with H&Y stage according to ANOVA (caudate: F=6.615, P<0.001; anterior putamen: F=2.316, P=0.081; posterior putamen: F=1.781, P=0.139). Additionally, the UPDRS III scores exhibited a significant increase with the progression of H&Y stages according to ANOVA (F=20.861; P<0.001) (*Table 4*).

Correlations between cerebral metabolism, dopaminergic function, and UPDRS scores in the early-iPD and late-iPD groups

In patients with early-iPD, the glucose metabolism correlated with UPDRS motor scores (putamen: r=0.343, P=0.030; globus pallidus: r=0.329, P=0.038) (*Figure 4A*). Additionally, the mean binding of ^{18}F-FP-DTBZ in the caudate (r=–0.425, P=0.011), anterior putamen (r=–0.471, P=0.004), and posterior putamen (r=–0.378, P=0.025) exhibited significant negative correlations with UPDRS motor scores (*Figure 4B*).

Similarly, in patients with late-stage iPD, the glucose metabolism in these brain regions correlated with UPDRS motor scores (putamen: r=0.240, P=0.021; globus pallidus: r=0.222, P=0.033) (*Figure 5A*). The average ^{18}F-FP-DTBZ binding in the caudate (r=–0.144; P=0.169), anterior putamen (r=–0.317, P=0.002), and posterior putamen (r=–0.298; P=0.004) also exhibited significant negative correlations with UPDRS motor scores (*Figure 5B*).

Discussion

The study examined the cerebral metabolism (^{18}F-FDG) and presynaptic dopaminergic function (^{18}F-FP-DTBZ) in patients with early-iPD or late-iPD. Additionally, the correlation between imaging measurements and clinical manifestations in these patients was also clarified. Our findings contribute to a greater understanding of the interplay between cerebral metabolism, dopaminergic function, and clinical assessments, providing a novel perspective on the distinct symptomatic profiles in individuals with early-iPD and late-iPD.

Early-iPD and late-iPD exhibit distinct clinical characteristics and disease course when categorized into subtypes solely based on age of onset. Late-iPD is associated with a faster disease progression, while early-iPD progresses more slowly (23). Therefore, analyzing the differences between early-iPD and late-iPD is critical to more meaningfully stratifying iPD subtypes for predicting disease progression (24). In line with previous studies (25), we observed that the late-iPD group had worse total UPDRS scores, MMSE scores, and MoCA scores as compared to the early-iPD group.

© AME Publishing Company.

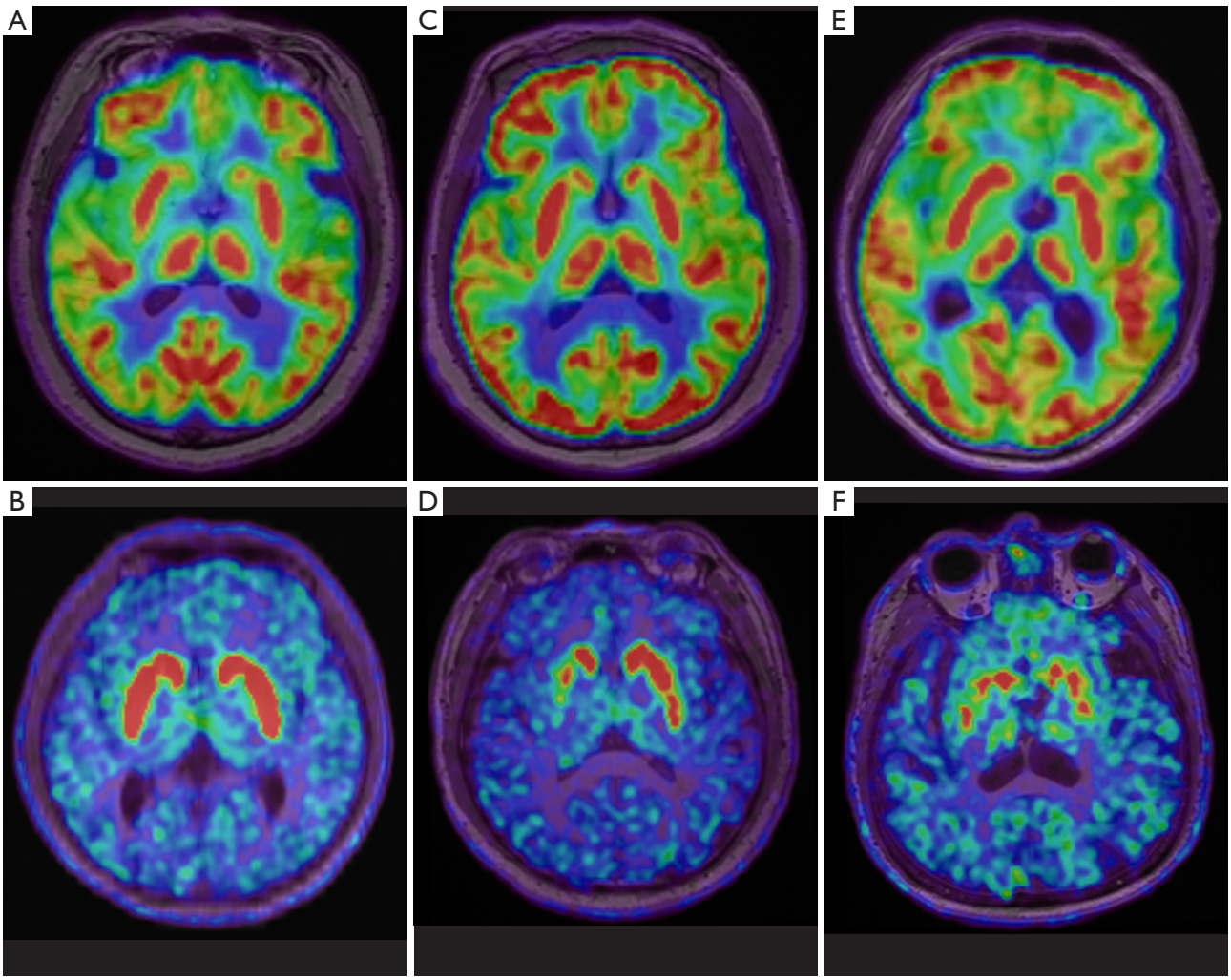

Figure 2 The images of ^{18}F-FDG and ^{18}F-FP-DTBZ PET/MR in healthy control participant (A,B) and patient with early-iPD (C,D), and patient with late-iPD (E,F). (A) ^{18}F-FDG PET/MR demonstrated a symmetrical distribution pattern across the entire cerebral cortex and nigrostriatal regions, showing no noticeable areas of increased or decreased radioactive uptake. (B) ^{18}F-FP-DTBZ PET-MR revealed a symmetrical distribution pattern, with the highest uptake in the striatal regions and moderate uptake in the substantia nigra. (C,D) A 73-year-old male patient with early-iPD. (C) ^{18}F-FDG PET-MR demonstrated metabolic reduction in the temporal cortex and increased metabolism in the putamen. (D) ^{18}F-FP-DTBZ PET/MR revealed a noticeable asymmetric VMAT2 binding decline, with the greatest loss observed in the posterior putamen. (E,F) A 75-year-old female patient with late-iPD. (E) ^{18}F-FDG PET/MR imaging showed metabolic reduction. (F) ^{18}F-FP-DTBZ PET-MR revealed a significant VMAT2 binding decline in the contralateral caudate and anterior putamen. ^{18}F-FDG, ^{18}F-fluorodeoxyglucose; ^{18}F-FP-DTBZ, [^{18}F] 9-fluoropropyl-(+)-dihydrotetrabenazine; PET-MR, positron emission tomography-magnetic resonance; early-iPD, early-onset idiopathic Parkinson disease; late-iPD, late-onset idiopathic Parkinson disease.

The characteristics of cerebral metabolism and presynaptic dopaminergic function in early-iPD and late-iPD

Our metabolic imaging study revealed that the iPD group, in comparison to the HC group, displayed the characteristic Parkinson disease-related metabolic pattern, which is consistent with previous research (26-28). Furthermore, patients with late-iPD exhibited a noteworthy decrease in ^{18}F-FDG PET-observed metabolism in the frontal, parietal, and temporal cortex, along with decreases in the globus pallidus, putamen, thalamus, and cerebellum, compared to

© AME Publishing Company.

Table 3 The characteristics of ^{18}F-FP-DTBZ PET imaging in the early-iPD, late-iPD, and HC groups

Region	SUVR				P_1	P_2	P_3
	Young HCs	Older HCs	Early-iPD	Late-iPD			
Caudate							
Contralateral	5.20±1.3	4.28±1.5	3.16±1.2	2.63±0.7	<0.001*	<0.001*	0.020*
Ipsilateral	5.20±1.3	4.28±1.5	3.00±1.2	2.72±0.9	<0.001*	0.001*	0.244
Anterior putamen							
Contralateral	6.20±1.9	5.20±2.0	2.49±1.2	2.05±0.7	<0.001*	<0.001*	0.040*
Ipsilateral	6.20±1.9	5.20±2.0	2.11±1.0	2.37±0.9	<0.001*	<0.001*	0.225
Posterior putamen							
Contralateral	5.30±1.6	4.93±1.6	1.76±0.7	1.59±0.8	<0.001*	<0.001*	0.344
Ipsilateral	5.30±1.6	4.93±1.6	1.59±0.6	1.87±0.9	<0.001*	<0.001*	0.138

The data are presented as the mean ± standard deviation. P_1 indicates the P value for the comparison of the young HC and early-iPD groups. P_2 indicates the P value for the comparison of the older HC and late-iPD groups. P_3 indicates the P value for the comparison of the early-iPD and late-iPD groups. *, statistically significant differences (P<0.05). ^{18}F-FP-DTBZ, [^{18}F] 9-fluoropropyl-(+)-dihydrotetrabenazine; PET, positron emission tomography; early-iPD, early-onset idiopathic Parkinson disease; late-iPD, late-onset idiopathic Parkinson disease; SUVR, standardized uptake value ratio; HC, healthy control.

the patients in the early-iPD group.

Age has been shown to play a crucial role in the decline of dopaminergic neurons and the progression of PD (29,30). In our study, the results of dopaminergic function imaging showed that patients with late-iPD had relatively higher nigrostriatal dysfunction compared to patients with early-iPD, suggesting a more pronounced loss of dopamine neuronal activity. These findings are consistent with the results from other studies using ^{11}C-methyl-N-2β-carbomethoxy-3β-(4-fluorophenyl)-tropanel (^{11}C-CFT) PET imaging (31,32). When the effects of disease duration were controlled for, it was observed that the early-iPD group had higher caudate nucleus ^{18}F-FP-DTBZ uptake, indicating less damage to dopaminergic neurons. This suggests that early-iPD may progress at a slower rate (33). This observation is in line with the pathological features of PD, where the ventral lateral substantia nigra is most affected, and dopaminergic neurons are the most deficient. Moreover, the middle and posterior regions of the putamen often receive major projections from this affected area of the substantia nigra. Consequently, the lesion initially affects these regions of the putamen, progressing to involve the anterior putamen and caudate nucleus as the disease advances (34). Additionally, the increased uptake of ^{18}F-FP-DTBZ in the caudate nucleus of the early-iPD group indicates a less-severe impairment of the dopaminergic neurons in this region, resulting in slower disease progression.

Correlations among metabolic changes, dopaminergic deficit, and clinical ratings in early-iPD and late-iPD

In cerebral metabolic imaging, the areas implicated in the cortex-striatum-thalamus-cortex pathway exhibited correlations with motor ratings in both the early-iPD and late-iPD groups. The traditional motor control model, which highlights the basal ganglia's influence on cortical function, provides an explanation for rigidity and bradykinesia (35,36). Additionally, dopaminergic function in the striatal region was found to negatively correlate with the motor score, indicating reduced substantia nigra-striatal dopaminergic activity in patients with early-iPD and late-iPD. The inhibition of the "direct pathway" and activation of the "indirect pathway" lead to motor symptoms, including decreased movement and rigidity (37,38). Therefore, an extended disease duration and advanced H&Y stage correlate with elevated motor symptom scores.

This study involved several limitations that should be acknowledged. First, as we employed a single-center design

© AME Publishing Company.

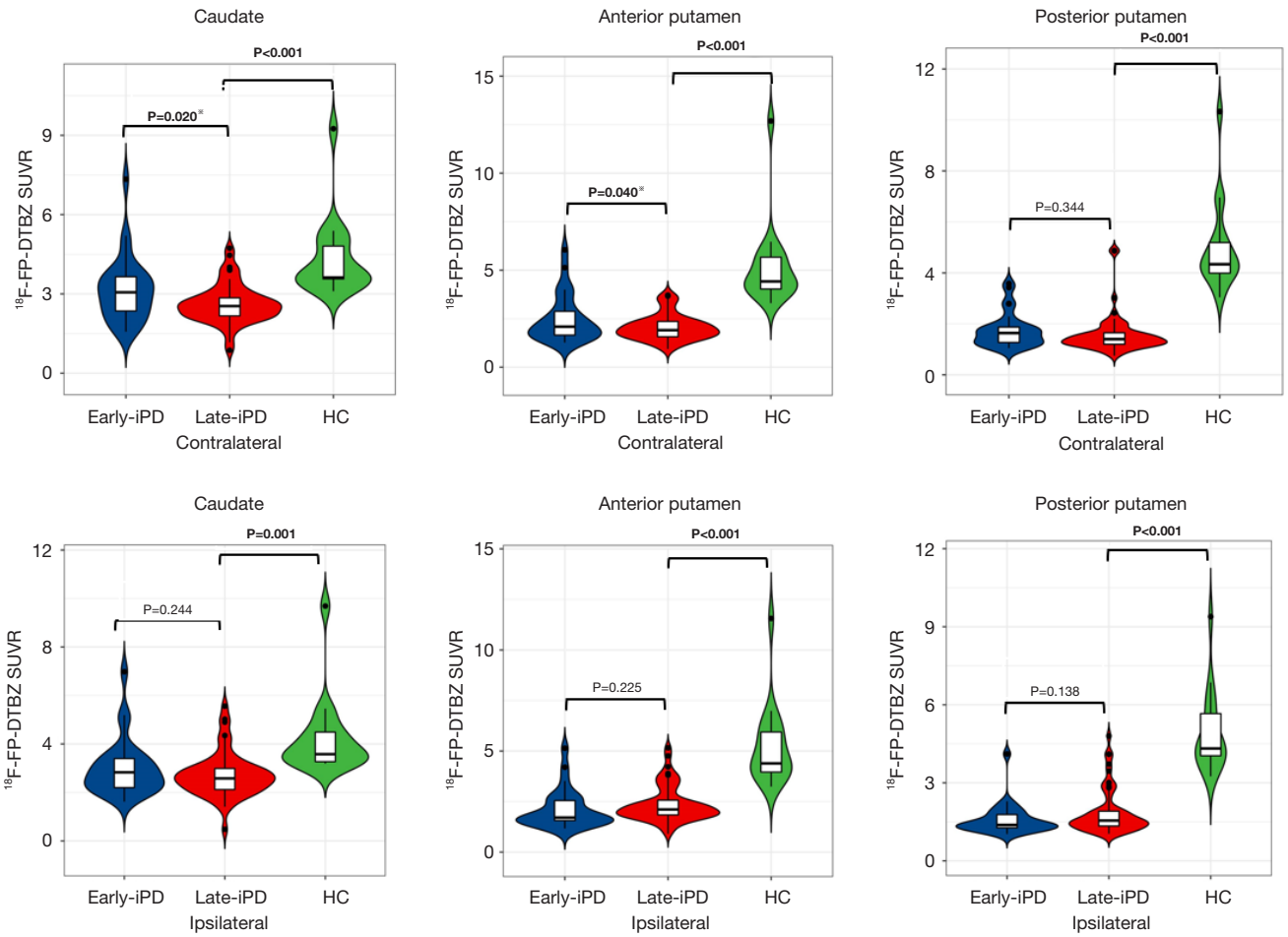

Figure 3 Comparative analysis of ^{18}F-FP-DTBZ uptake within the striatal regions of HC individuals and patients with early-iPD and late-iPD. In the-iPD group, the uptake of ^{18}F-FP-DTBZ showed a significant decline in the striatum regions as compared that in older HC group (P<0.001). Additionally, the ^{18}F-FP-DTBZ binding potential was significantly lower in the contralateral caudate and anterior putamen in the late-iPD group as compared to that in the early- iPD group (P<0.001). Bold indicates the statistically significant differences in the comparison between the older HC and late-iPD groups (P<0.05). ※ indicates statistically significant differences in the comparison between the early-iPD and late-iPD groups (P<0.05). ^{18}F-FP-DTBZ, [^{18}F] 9-fluoropropyl-(+)-dihydrotetrabenazine; SUVR, standardized uptake value ratio; early-iPD, early-onset idiopathic Parkinson disease; late-iPD, late-onset idiopathic Parkinson disease; HC, healthy control.

with a small sample size, biases related to geography, race, examination, and assessment might have been present. Therefore, expanding the sample size and transitioning to a multicenter approach is recommended to enhance the study's credibility. Second, the results may be influenced by the state of cognitive decline and emotional factors (39-41), while the assessment of VMAT2 binding may be influenced by normal aging (42,43), potentially leading to an overestimation of disease severity.

Conclusions

^{18}F-FDG and ^{18}F-FP-DTBZ PET offer an objective molecular imaging basis for distinguishing between patients with early-iPD and those with late-iPD. Additionally, correlation analysis between imaging and clinical data provides a new approach for exploring the potential applications in future studies that examine early-iPD and late-iPD.

© AME Publishing Company.

Table 4 Comparison of cerebral metabolism, dopaminergic function, and H&Y stages between the early-iPD and late-iPD groups

Region	Early-iPD		Late-iPD	
	F	P	F	P
^{18}F-FDG				
Putamen	5.146	0.007*	3.190	0.046*
Globus pallidus	3.620	0.034*	3.807	0.026*
^{18}F-FP-DTBZ				
Caudate	9.228	<0.001*	6.615	<0.001*
Anterior putamen	9.577	<0.001*	2.316	0.081
Posterior putamen	4.916	0.012*	1.781	0.139

*, statistically significant differences (P<0.05). H&Y stage, Hoehn-Yahr stage; early-iPD, early-onset idiopathic Parkinson disease; late-iPD, late-onset idiopathic Parkinson disease; ^{18}F-FDG, ^{18}F-fluorodeoxyglucose; ^{18}F-FP-DTBZ, [^{18}F] 9-fluoropropyl-(+)-dihydrotetrabenazine.

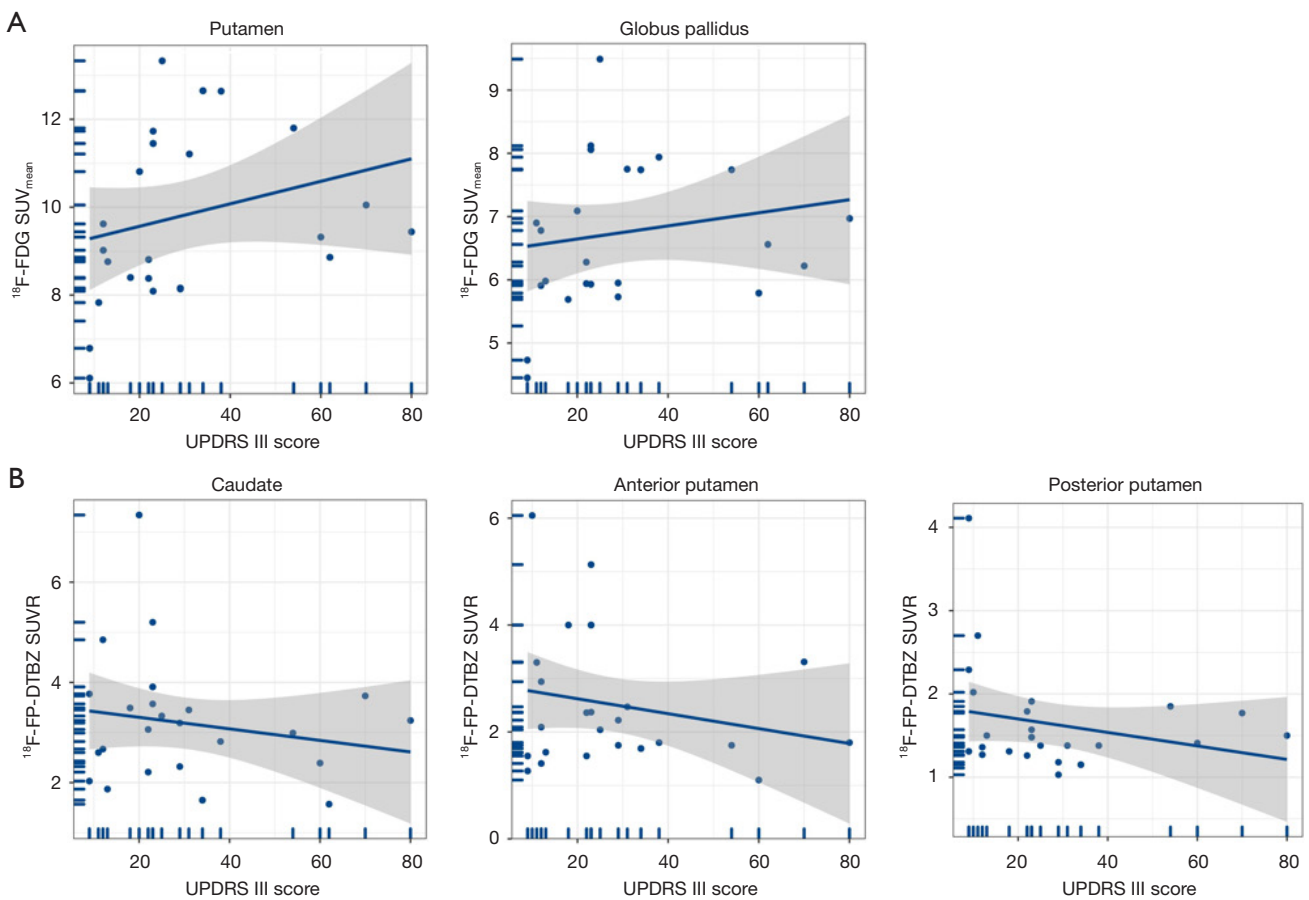

Figure 4 Correlation of glucose metabolism and ^{18}F-FP-DTBZ binding with UPDRS motor scores in the early-iPD group. (A) The correlations of glucose metabolism in the putamen and globus pallidus with UPDRS III scores. (B) The correlations of ^{18}F-FP-DTBZ binding (ROIs) in the caudate, anterior putamen, and posterior putamen with UPDRS III scores. SUV, standardized uptake value; ^{18}F-FDG, ^{18}F-fluorodeoxyglucose; UPDRS III, Unified Parkinson Disease Rating Scale Part III; ^{18}F-FP-DTBZ, [^{18}F] 9-fluoropropyl-(+)-dihydrotetrabenazine; early-iPD, early-onset idiopathic Parkinson disease; ROI, region of interest.

© AME Publishing Company.

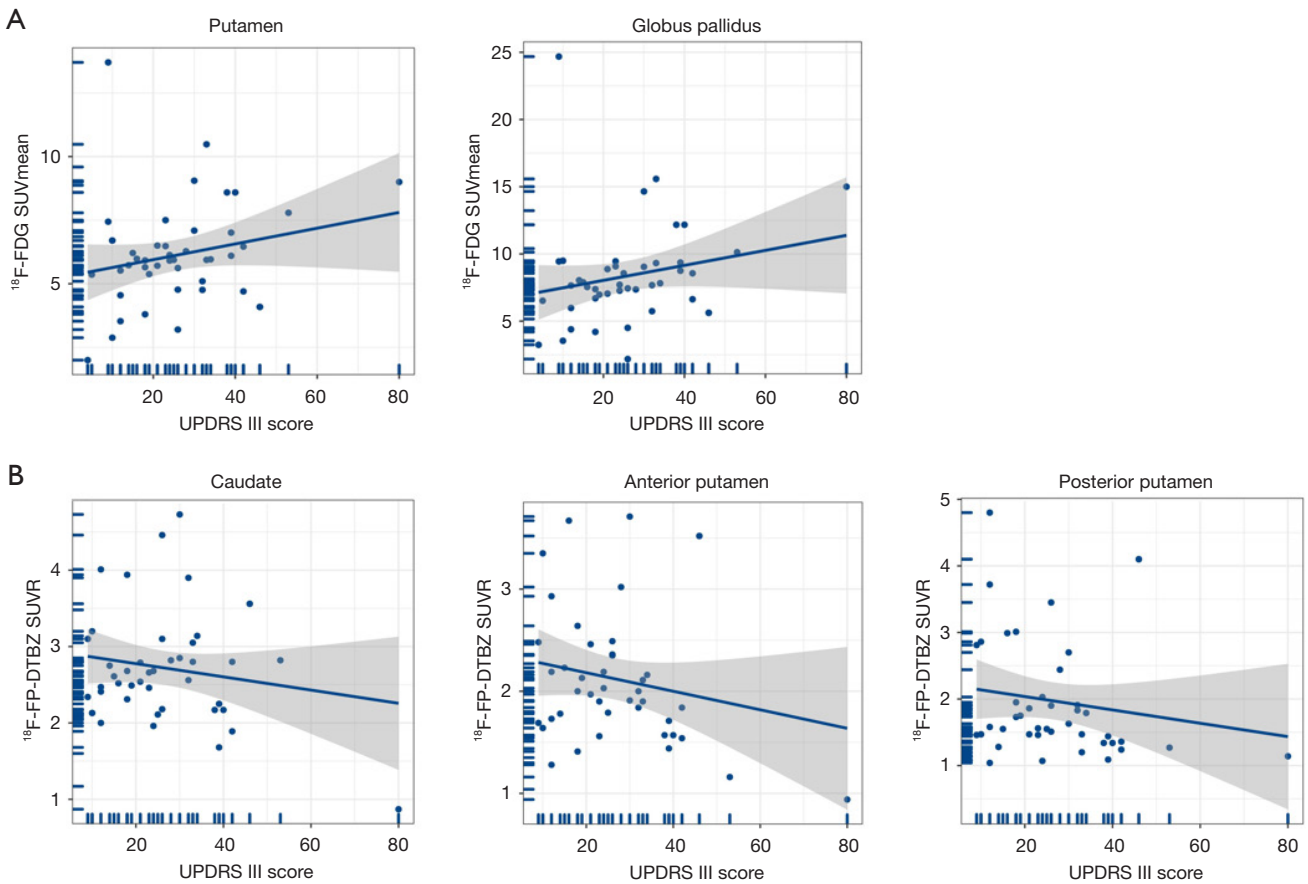

Figure 5 Correlation of glucose metabolism and ^{18}F-FP-DTBZ binding with UPDRS motor scores in the late-iPD group. (A) The correlations of glucose metabolism in putamen and globus pallidus with UPDRS III scores. (B) The correlations of ^{18}F-FP-DTBZ binding (ROIs) in the caudate, anterior putamen, and posterior putamen with UPDRS III scores. SUV, standardized uptake value; ^{18}F-FDG, ^{18}F-fluorodeoxyglucose; UPDRS III, Unified Parkinson Disease Rating Scale Part III; ^{18}F-FP-DTBZ, [^{18}F] 9-fluoropropyl-(+)-dihydrotetrabenazine; SUVR, standardized uptake value ratio; late-iPD, late-onset idiopathic Parkinson disease; ROI, region of interest

Acknowledgments

Funding: This work was supported by the National Key Research and Development Program of China (Nos. 2022YFC2406900 and 2022YFC2406904).

Footnote

Reporting Checklist: The authors have completed the STROBE reporting checklist. Available at https://qims.amegroups.com/article/view/10.21037/qims-24-804/rc

Conflicts of Interest: All authors have completed the ICMJE uniform disclosure form (available at https://qims.amegroups.com/article/view/10.21037/qims-24-804/coif). This work was supported by the National Key Research and Development Program of China (Nos. 2022YFC2406900 and 2022YFC2406904). The authors have no other conflicts of interest to declare.

Ethical Statement: The authors are accountable for all aspects of the work in ensuring that questions related to the accuracy or integrity of any part of the work are appropriately investigated and resolved. This retrospective study was conducted in accordance with the Declaration of Helsinki (as revised in 2013) and was approved by the Medical Research Ethics Committee of Xuanwu Hospital, Capital Medical University (No. [2023]044). The requirement for written informed consent was waived due to the retrospective nature of the analysis.

© AME Publishing Company.

Open Access Statement: This is an Open Access article distributed in accordance with the Creative Commons Attribution-NonCommercial-NoDerivs 4.0 International License (CC BY-NC-ND 4.0), which permits the non-commercial replication and distribution of the article with the strict proviso that no changes or edits are made and the original work is properly cited (including links to both the formal publication through the relevant DOI and the license). See: https://creativecommons.org/licenses/by-nc-nd/4.0/.

References

1. Tolosa E, Garrido A, Scholz SW, Poewe W. Challenges in the diagnosis of Parkinson's disease. Lancet Neurol 2021;20:385-97.
2. Vijiaratnam N, Simuni T, Bandmann O, Morris HR, Foltynie T. Progress towards therapies for disease modification in Parkinson's disease. Lancet Neurol 2021;20:559-72.
3. Emamzadeh FN, Surguchov A. Parkinson's Disease: Biomarkers, Treatment, and Risk Factors. Front Neurosci 2018;12:612.
4. Dickson DW. Neuropathology of Parkinson disease. Parkinsonism Relat Disord 2018;46 Suppl 1:S30-3.
5. Maristany AJ, Sa BC, Murray C, Subramaniam AB, Oldak SE. Psychiatric Manifestations of Neurological Diseases: A Narrative Review. Cureus 2024;16:e64152.
6. Qian E, Huang Y. Subtyping of Parkinson's Disease - Where Are We Up To? Aging Dis 2019;10:1130-9.
7. De Carolis L, Galli S, Bianchini E, Rinaldi D, Raju M, Caliò B, Alborghetti M, Pontieri FE. Age at Onset Influences Progression of Motor and Non-Motor Symptoms during the Early Stage of Parkinson's Disease: A Monocentric Retrospective Study. Brain Sci 2023;13:157.
8. Mehanna R, Smilowska K, Fleisher J, Post B, Hatano T, Pimentel Piemonte ME, Kumar KR, McConvey V, Zhang B, Tan EK, Savica R; . Age Cutoff for Early-Onset Parkinson's Disease: Recommendations from the International Parkinson and Movement Disorder Society Task Force on Early Onset Parkinson's Disease. Mov Disord Clin Pract 2022;9:869-78.
9. Angelopoulou E, Bozi M, Simitsi AM, Koros C, Antonelou R, Papagiannakis N, Maniati M, Poula D, Stamelou M, Vassilatis DK, Michalopoulos I, Geronikolou S, Scarmeas N, Stefanis L. Clinical differences between early-onset and mid-and-late-onset Parkinson's disease: Data analysis of the Hellenic Biobank of Parkinson's disease. J Neurol Sci 2022;442:120405.
10. Zhou Z, Zhou X, Xiang Y, Zhao Y, Pan H, Wu J, Xu Q, Chen Y, Sun Q, Wu X, Zhu J, Wu X, Li J, Yan X, Guo J, Tang B, Lei L, Liu Z. Subtyping of early-onset Parkinson's disease using cluster analysis: A large cohort study. Front Aging Neurosci 2022;14:1040293.
11. Pagano G, Ferrara N, Brooks DJ, Pavese N. Age at onset and Parkinson disease phenotype. Neurology 2016;86:1400-7.
12. Liu FT, Ge JJ, Wu JJ, Wu P, Ma Y, Zuo CT, Wang J. Clinical, Dopaminergic, and Metabolic Correlations in Parkinson Disease: A Dual-Tracer PET Study. Clin Nucl Med 2018;43:562-71.
13. Palermo G, Giannoni S, Frosini D, Morganti R, Volterrani D, Bonuccelli U, Pavese N, Ceravolo R. Dopamine Transporter, Age, and Motor Complications in Parkinson's Disease: A Clinical and Single-Photon Emission Computed Tomography Study. Mov Disord 2020;35:1028-36.
14. Postuma RB, Berg D, Stern M, Poewe W, Olanow CW, Oertel W, Obeso J, Marek K, Litvan I, Lang AE, Halliday G, Goetz CG, Gasser T, Dubois B, Chan P, Bloem BR, Adler CH, Deuschl G. MDS clinical diagnostic criteria for Parkinson's disease. Mov Disord 2015;30:1591-601.
15. Postuma RB, Poewe W, Litvan I, Lewis S, Lang AE, Halliday G, Goetz CG, Chan P, Slow E, Seppi K, Schaffer E, Rios-Romenets S, Mi T, Maetzler C, Li Y, Heim B, Bledsoe IO, Berg D. Validation of the MDS clinical diagnostic criteria for Parkinson's disease. Mov Disord 2018;33:1601-8.
16. Wu W, Gong S, Wang S, Lei W, Yuan L, Wu W, Qiu J, Sun W, Luan G, Zhu M, Wang X, Liang G, Tao Y. Safety and efficiency of deep brain stimulation in the elderly patients with Parkinson's disease. CNS Neurosci Ther 2024;30:e14899.
17. Scheperjans F, Levo R, Bosch B, Lääperi M, Pereira PAB, Smolander OP, Aho VTE, Vetkas N, Toivio L, Kainulainen V, Fedorova TD, Lahtinen P, Ortiz R, Kaasinen V, Satokari R, Arkkila P. Fecal Microbiota Transplantation for Treatment of Parkinson Disease: A Randomized Clinical Trial. JAMA Neurol 2024;81:925-38.
18. Wu J, Yang M, Zhang Y, Ren YK, Ding CW, Ying CC, Wu QR, Wang CS, Sheng YJ, Mao P, Chen XF, Zhang YC, Liu CF. Changes in the correlation between substantia nigra hyperechogenicity area and Parkinson's disease severity at different Hoehn and Yahr stages. Neurol Sci 2024. [Epub ahead of print]. doi: 10.1007/s10072-024-07697-0.

19. Hong Y, Fu C, Xing Y, Tao J, Zhao T, Wang N, Chen Y, You Y, Ren Z, Hong Y, Wang Q, Zhao Y, Yang Y, Zhang J, Xu J, Han X. Delayed (18)F-FDG PET imaging provides better metabolic asymmetry in potential epileptogenic zone in temporal lobe epilepsy. Front Med (Lausanne) 2023;10:1180541.
20. Shi X, Gu Q, Fu C, Ma J, Li D, Zheng J, Chen S, She Z, Qi X, Li X, Wu S, Wang L. Relationship of irisin with disease severity and dopamine uptake in Parkinson's disease patients. Neuroimage Clin 2024;41:103555.
21. Lin SC, Lin KJ, Hsiao IT, Hsieh CJ, Lin WY, Lu CS, Wey SP, Yen TC, Kung MP, Weng YH. In vivo detection of monoaminergic degeneration in early Parkinson disease by (18)F-9-fluoropropyl-(+)-dihydrotetrabenzazine PET. J Nucl Med 2014;55:73-9.
22. Hsiao IT, Weng YH, Hsieh CJ, Lin WY, Wey SP, Kung MP, Yen TC, Lu CS, Lin KJ. Correlation of Parkinson disease severity and 18F-DTBZ positron emission tomography. JAMA Neurol 2014;71:758-66.
23. Fereshtehnejad SM, Postuma RB. Subtypes of Parkinson's Disease: What Do They Tell Us About Disease Progression? Curr Neurol Neurosci Rep 2017;17:34.
24. Ren J, Zhan X, Zhou H, Guo Z, Xing Y, Yin H, Xue C, Wu J, Liu W. Comparing the effects of GBA variants and onset age on clinical features and progression in Parkinson's disease. CNS Neurosci Ther 2024;30:e14387.
25. Yoon SY, Lee SC, Suh JH, Yang SN, Han K, Kim YW. Different risks of early-onset and late-onset Parkinson disease in individuals with mental illness. NPJ Parkinsons Dis 2024;10:17.
26. Meles SK, Renken RJ, Pagani M, Teune LK, Arnaldi D, Morbelli S, Nobili F, van Laar T, Obeso JA, Rodríguez-Oroz MC, Leenders KL. Abnormal pattern of brain glucose metabolism in Parkinson's disease: replication in three European cohorts. Eur J Nucl Med Mol Imaging 2020;47:437-50.
27. Rus T, Schindlbeck KA, Tang CC, Vo A, Dhawan V, Trošt M, Eidelberg D. Stereotyped Relationship Between Motor and Cognitive Metabolic Networks in Parkinson's Disease. Mov Disord 2022;37:2247-56.
28. Shin JH, Lee JY, Kim YK, Yoon EJ, Kim H, Nam H, Jeon B. Parkinson Disease-Related Brain Metabolic Patterns and Neurodegeneration in Isolated REM Sleep Behavior Disorder. Neurology 2021;97:e378-88.
29. Yan S, Lu J, Zhu H, Tian T, Qin Y, Li Y, Zhu W. The influence of accelerated brain aging on coactivation pattern dynamics in Parkinson's disease. J Neurosci Res 2024;102:e25357.
30. Alzate Sanchez AM, Janssen MLF, Temel Y, Roberts MJ. Aging suppresses subthalamic neuronal activity in patients with Parkinson's disease. Eur J Neurosci 2024. [Epub ahead of print]. doi: 10.1111/ejn.16435.
31. Yang YJ, Ge JJ, Liu FT, Liu ZY, Zhao J, Wu JJ, Ma Y, Zuo CT, Wang J. Preserved caudate function in young-onset patients with Parkinson's disease: a dual-tracer PET imaging study. Ther Adv Neurol Disord 2019;12:1756286419851400.
32. Kangli F, Hongguang Z, Yinghua L, Xiaoxiao D, Yuyin D, Lulu G, Yi L, Zhihui S, Ying Z. Characteristics and influencing factors of (11)C-CFT PET imaging in patients with early and late onset Parkinson's disease. Front Neurol 2023;14:1195577.
33. Lee MJ, Pak K, Kim HK, Nudelman KN, Kim JH, Kim YH, Kang J, Baek MS, Lyoo CH. Genetic factors affecting dopaminergic deterioration during the premotor stage of Parkinson disease. NPJ Parkinsons Dis 2021;7:104.
34. Liu XL, Liu SY, Barret O, Tamagnan GD, Qiao HW, Song TB, Lu J, Chan P. Diagnostic value of striatal (18) F-FP-DTBZ PET in Parkinson's disease. Front Aging Neurosci 2022;14:931015.
35. Shang S, Wang L, Yao J, Lv X, Xu Y, Dou W, Zhang H, Ye J, Chen YC. Characterizing microstructural patterns within the cortico-striato-thalamo-cortical circuit in Parkinson's disease. Prog Neuropsychopharmacol Biol Psychiatry 2024;135:111116.
36. DeLong MR, Wichmann T. Basal Ganglia Circuits as Targets for Neuromodulation in Parkinson Disease. JAMA Neurol 2015;72:1354-60.
37. Poewe W, Seppi K, Tanner CM, Halliday GM, Brundin P, Volkmann J, Schrag AE, Lang AE. Parkinson disease. Nat Rev Dis Primers 2017;3:17013.
38. Miocinovic S, Somayajula S, Chitnis S, Vitek JL. History, applications, and mechanisms of deep brain stimulation. JAMA Neurol 2013;70:163-71.
39. Alfano V, Longarzo M, Mele G, Esposito M, Aiello M, Salvatore M, Grossi D, Cavaliere C. Identifying a Common Functional Framework for Apathy Large-Scale Brain Network. J Pers Med 2021;11:679.
40. Narme P, Mouras H, Roussel M, Duru C, Krystkowiak P, Godefroy O. Emotional and cognitive social processes are impaired in Parkinson's disease and are related to behavioral disorders. Neuropsychology 2013;27:182-92.
41. Alfano V, Federico G, Mele G, Garramone F, Esposito M, Aiello M, Salvatore M, Cavaliere C. Brain Networks Involved in Depression in Patients with Frontotemporal Dementia and Parkinson's Disease: An Exploratory

© AME Publishing Company.

Resting-State Functional Connectivity MRI Study. Diagnostics (Basel) 2022.
42. Lin KJ, Weng YH, Hsieh CJ, Lin WY, Wey SP, Kung MP, Yen TC, Lu CS, Hsiao IT. Brain imaging of vesicular monoamine transporter type 2 in healthy aging subjects by 18F-FP-(+)-DTBZ PET. PLoS One 2013;8:e75952.
43. Troiano AR, Schulzer M, de la Fuente-Fernandez R, Mak E, McKenzie J, Sossi V, McCormick S, Ruth TJ, Stoessl AJ. Dopamine transporter PET in normal aging: dopamine transporter decline and its possible role in preservation of motor function. Synapse 2010;64:146-51.

Cite this article as: Li S, Lu W, Yan S, Song T, Zhang C, Yang C, Lu J. The combination of ^{18}F-fluorodeoxyglucose and ^{18}F 9-fluoropropyl-(+)-dihydrotetrabenazine positron emission tomography for distinguishing between early-onset and late-onset idiopathic Parkinson disease and analyzing influencing factors. Quant Imaging Med Surg 2024;14(10):7406-7419. doi: 10.21037/qims-24-804

© AME Publishing Company.